DOE/ER/60658--4

DE92 003695

Annual Progress Report

Mutagenicity of Radon and Radon Daughters

Helen H. Evans

Case Western Reserve University

RADON GENERATOR

New Design for the Generator

The design of the radon generator was changed from the one described in the original application. The changes were made in order to eliminate all glass and plastic components, and thus avoid the use of any fragile or radiation-degradable parts. The new design uses components of aluminum, brass and copper. The activity of the radium in the generator was increased from the original 10 millicuries to nearly 80 millicuries. This will provide much greater flexibility in the choice of radiation doses and dose rates. Figure 1 is a photograph of the new generator, and Figure 2 illustrates its main parts. The largest part, A, was machined from a solid aluminum cylinder of diameter 4-1/2" (114 mm) and length 3" (76 mm), in which a cavity 2-1/4" (57 mm) deep and 2" (51 mm) in diameter was bored. Threads were cut into the inner side as shown.

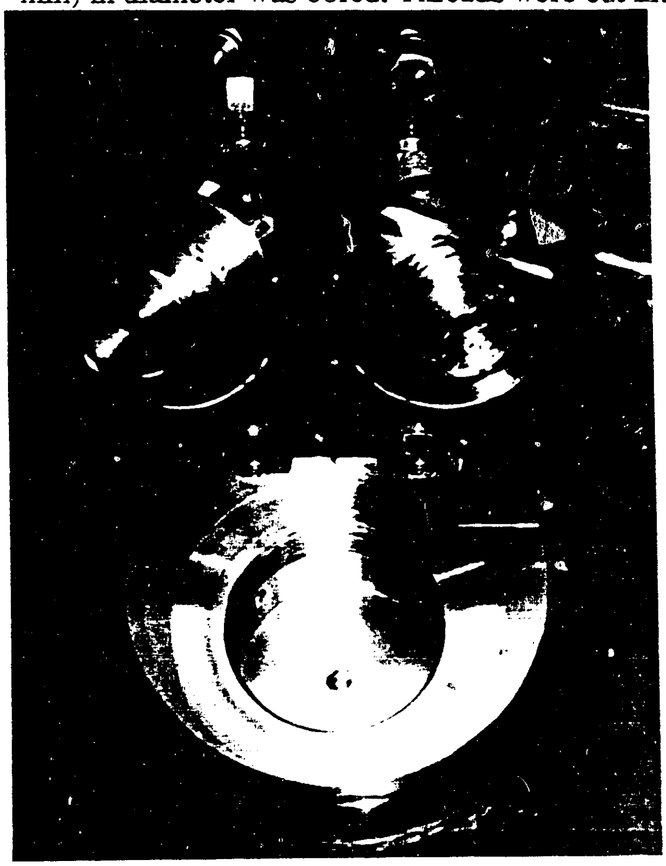

Fig. 1

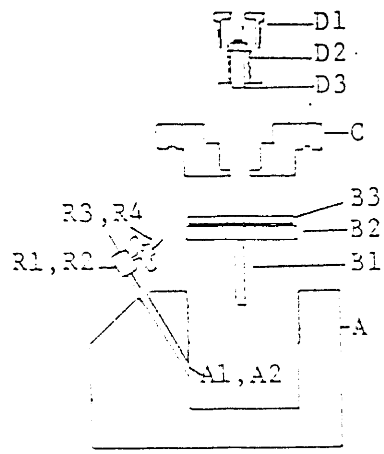

Fig. 2

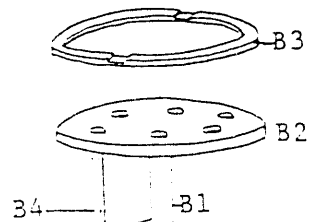

Fig. 3

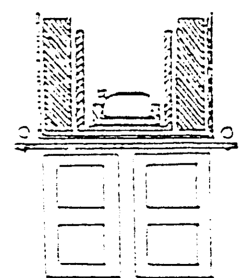

Fig. 4

Within the enclosure so formed, an aluminum disk B2 of thickness 1/8" (3 mm) was screwed in until the attached 1-1/4" (32 mm) long shaft B1 touched the bottom. The disk lay approximately half-way between the top and bottom of the cavity. Figure 3 shows a more detailed illustration of this part. Resting on the disk was a ring B3 of nearly the same diameter. Two notches 3/16" (5 mm) wide were cut into it at opposite sides. These dimensions were chosen to accomodate a glass capsule containing radium salt that now serves as the radon source. Six small holes of diameter 1/4" (6 mm) were drilled through the disk to permit mixing of the gas above and below it. A vane B4 was mounted into a slot cut into the shaft and was aligned between the two holes A1 and A2 (see Figure 2) leading out of the enclosure. The presence of the vane promotes mixing of the gas inside the enclosure during use, when one hole serves as an inlet and the other as an outlet. In the final arrangement, a single layer of fine copper mesh was laid over the retaining ring B3, and the radium capsule placed on the mesh. Its purpose was to confine the radium salt and glass fragments from the capsule to the upper half of the chamber and prevent them from entering the holes A1 and A2.

An aluminum lid C was screwed onto the top of the enclosure with "silver goop", an anti-sieze compound, coated on the threads. The lid was designed to facilitate breaking of the radium-containing glass capsule after the enclosure had been made air-tight. This was achieved by the use of a Hoke bellows valve (illustrated as D1 and D2 in Figure 2) mounted and sealed into the center of the lid. The dimensions were carefully chosen so that when the lid was screwed on the generator to make a tight fit, the bottom of the stem D3 would be approximately 2 mm above the glass capsule resting on the ring B3. The capsule was fractured by pushing the stem down on it.

The air-tightness of the generator was ensured by the use of an indium gasket. An O-ring groove was cut into the bottom surface of the lid and lined with indium wire of diameter 0.064" (1.6 mm). Indium was chosen in preference to copper since the former has better sealing characteristics than copper which requires a stainless steel knife edge to effect sealing. Radon gas was withdrawn from hole A1 as air was pumped into A2. Access to the valves was controlled by two Nupro bellows valves of brass (R1 and R2 in Figure 2), guaranteed by the manufacturer to have been helium leak-tested to 4 x 10^{-9} atm cc/sec. Three-foot flexible cables (R3, R4) were mounted on the valve controls to permit manipulation of the valves from a safe distance. Copper tubing (diameter 1/8") was connected to the valves and terminated in a Whitey 4-way cross-over ball valve made of brass (not shown in Figure 2), which therefore served as a secondary barrier to radon leakage or diffusion.

Figure 4 shows the generator in its containment assembly. The generator was placed in a shallow plastic dish and was immobilized by Cerrobend alloy that was poured around it. Both were housed in a box constructed of overlapping lead plates. Two adjacent walls were 1" (25 mm) thick and the other two were 1/4" (6 mm) thick. In the final position the box was oriented so that the thinner walls were directed towards concrete barriers. The bottom and top were 1/2" and 1" (13 and 25 mm) thick respectively. The lead box was placed inside a large 12" x 12 x 12" (30 cm x 30 cm x 30 cm) polypropylene box, and all intervening space was filled with lead bricks. This rested on a 1/2" (13 mm) aluminum plate, which in turn rested on four concrete blocks inside a large concrete sink. The aluminum plate was fitted with four eye-bolts at the corners and a 3/8" (10 mm) link chain was run through them. There was enough slack in the chain so that, if necessary, it could be gathered up and passed over a 1" (25 mm) steel rod above the polypropylene box. The entire assembly, weighing about 400 lb (180 kg), could then be lifted by a ceiling-mounted crane rated for 1/4 ton (220 kg) loads. Thus in the event of an irretrievable impairment of the generator, the whole assembly could be lifted and placed inside a steel drum adjacent to the concrete sink.

Loading the Generator with Radium

Prior to loading the generator with the radium, it was tested for its air-tightness. With the generator empty, the lid was fitted with an indium gasket and screwed on until it was tight. It was further tightened at intervals of 2 to 3 hours to permit the indium to flow between each tightening. The volume within the generator was then raised to about 100 torr above barometric pressure by activating a pump (described below). A mercury manometer enabled the exact pressure to be determined. The Nupro bellows valves were closed and the pressure was measured again after intervals of a few hours, a day and several days. It was determined to our satisfaction that the generator exhibited no detectable leakage. When we were ready to proceed with the loading, the site of the generator was prepared with suitable padding the groove in the lid was fitted with a new indium gasket. The capsule containing the radium was carefully transferred to the generator and aligned with the slots in the retaining ring. The cap was screwed on until it was snug. An alpha scintillation detector (Ludlum Model 43-2) was used to check for contamination around the generator, and none was found. The lid was further tightened over a period of 7 days. The pressure check was conducted during this time using the pump and mercury manometer. When all signs were satisfactory, the plunger on the Hoke bellows valve was depressed and the capsule broken.

Radon Delivery Apparatus

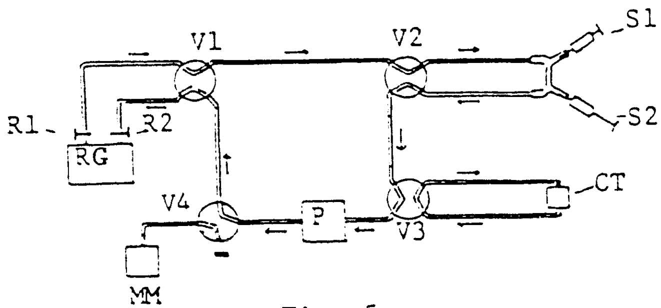

Fig. 5

Figure 5 shows the various components of the radon delivery apparatus. They consist of the radon generator (RG), the two Nupro valves (R1 and R2), the brass cross-over ball valve V1, three Omnifit four-way valves V2, V3 and V4, a pump P, and an arm to which can be fitted two syringes S1 and S2. The syringe needles are inserted through tight-fitting rubber septa. S1 is the syringe into which radon gas is drawn while S2 acts as an air reservoir to replenish the gas within the system. All tubing is of 1/8" copper or Tygon. The valve V4 is used only when the pressure in the system is to be determined. Normally it is left in the position shown. When radon loading is about to commence, the two valves R1 and R2 are opened and V1 is turned to the position shown in Figure 5. Valves V2, V3 and V4 are already in the positions shown. The pump is started so as to move gas through the system Thirty seconds are allowed to elapse to permit the radon to reach the delivery area. The plunger in S1 is withdrawn while that on S2 is allowed to move inwards. An adequate volume of gas (5 to 10 ml) is drawn over a period of about 1/2 minute, and the syringe is removed. The pump is then switched off, valves R1 and R2 are closed, and V1 is turned so that the generator is isolated. Valve V3 is turned so that the charcoal trap is included in the circuit. The pump is switched on again and run for 10 minutes so that all remaining radon in the tubing is driven through the activated charcoal to be adsorbed there. The radon in S1 is injected immediately into one or more flasks containing tissue culture medium, which are then sealed with grease, enclosed in plastic bags, and set aside to reach radioactive equilibrium. The delivery system is under a canopy with plastic sheets around it so as to simulate a small fume hood. Air is pulled from the canopy by a 1/2 horsepower pump, passed through an activated charcoal bed and ejected into an exhaust stainless steel duct. The pump is operated on an emergency backup power circuit.

Dose Rates Obtained Following Injection of Radon Gas Mixture

Different amounts of the radon-containing gas mixture were withdrawn into the syringe and delivered to the gas phase above 100 ml of cell culture medium in a series of spinner flasks. After four hours when equilibrium was attained, samples of the medium were withdrawn and the radioactivity determined. The dose rate to the cells due the radioactivity of the medium was then determined as described previously. The radioactivity of the medium and the subsequent dose rate were proportional to the amount of radon-containing gas mixture injected. For 30 different injections of 1-24 ml of gas mixture, an average dose rate of 0.026 Gy/hr was obtained per ml of radon gas mixture injected. Using this system we will easily be able to vary the dose rate delivered to the cells.

Dosimetry

The dose to the cells is determined from the radioactivity of the medium as well as from the radon daughters attached to the cells (Jostes *et al.*, Radiation Research, in press). The dose from the medium is calculated from the γ radioactivity emitted by 214-Bi, as described previously. The amount of short-lived α-emitting radon daughters attached to the L5178Y cells as a function of time and of the α radioactivity in the medium have been determined with radon obtained from the new radon generator. Attachment of the radon daughters to the cells was proportional to the radioactivity of the medium as shown in Fig. 6. Attachment also increased with time for approximately 3 hours, remained constant until 7.5 hours, and then decreased, as shown in Fig. 7. The attachment of the radon daughters did not differ significantly for strains LY-R16 and LY-S1. These results will be used to determine the total dose to the cell nucleus, as we have determined previously for CHO cells (Jostes *et al., ibid.*).

Fig. 6: Attachment of Radon Daughters to Cells vs. Medium Radioactivity

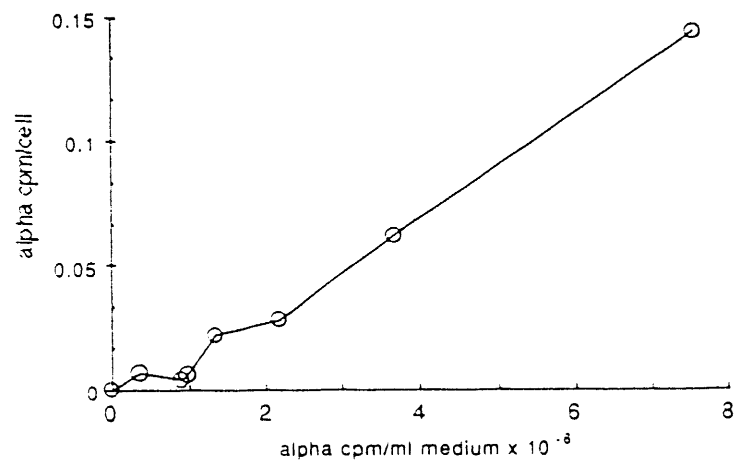

Figure 7. Attachment of Rn Daughters vs. Time

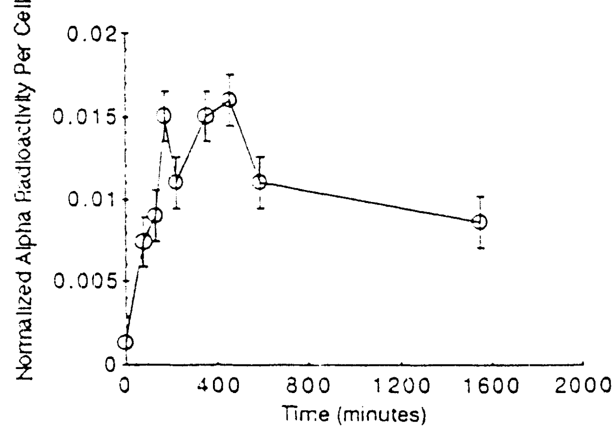

The Nature of the Radon-Induced Lesion Inactivating the Thymidine Kinase (*tk*) Gene in L5178Y Cell.

As reported last year, we found that 84% of radon-induced $TK^{-/-}$ mutants had lost the entire active *tk* allele. The extension of the lesion inactivating the *tk* gene to the neighboring galactokinase (*gk*) gene (within 200 kb of the *tk* gene) was assessed by determining galactokinase (GK) activity in homogenates of the $TK^{-/-}$ mutants. We found that approximately half of the TK-/- mutants of strains LY-R16 and LY-S1 showed inactivation of GK, indicating that an intergenic deletion had occurred. The extension of the lesion to the *gk* gene has been compared in $TK^{-/-}$ mutants induced by radon and radon daughters, by X radiation, and by UV radiation. The results are shown in Fig. 8.

Fig. 8. Loss of Galactokinase Activity in $TK^{-/-}$ Mutants Induced by Various Agents

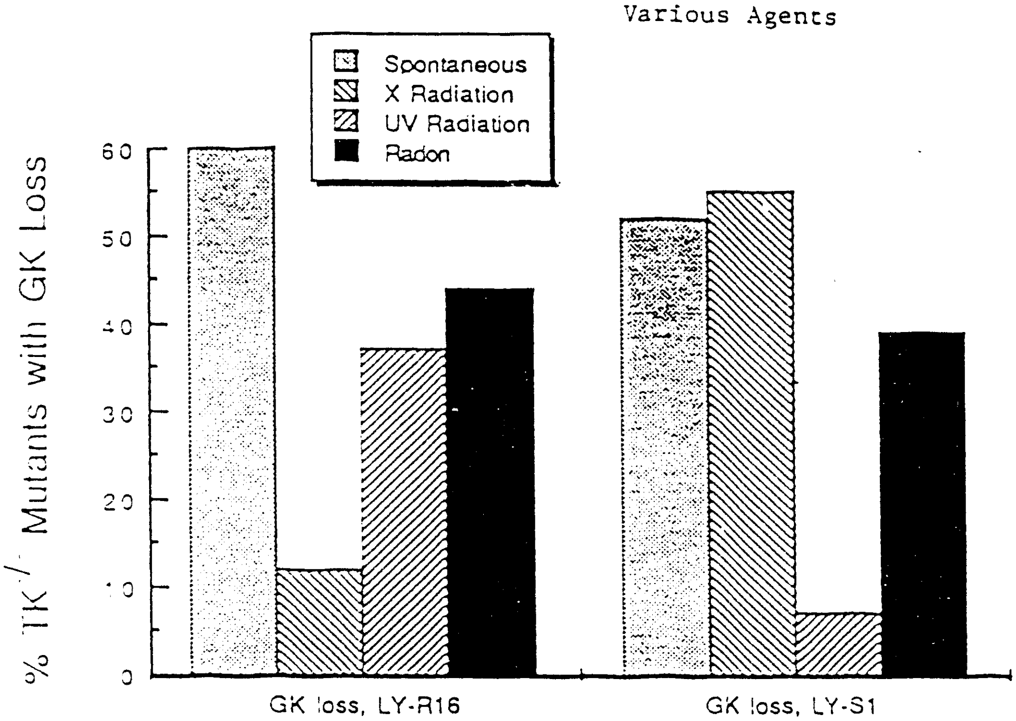

It appears that a greater proportion of $TK^{-/-}$ mutants show GK inactivation under conditions when DNA repair is deficient. Strain LY-S1 is deficient in the repair of ionizing radiation-induced double-strand breaks, and a greater percentage of X radiation-induced mutants of strain LY-S1 show inactivation of GK than for strain LY-R16 which is proficient in double-strand break repair. Strain LY-R16 is deficient in DNA excision repair, and a greater proportion of UV radiation-induced mutants of strain LY-R16 show inactivation of GK than in the case of strain LY-S1 which is proficient in excision repair. Radon-induced DNA lesions are thought to be irreparable in both strains, and a large proportion of the $TK^{-/-}$ mutants of both strains show GK inactivation. These results indicate that a deficiency in DNA repair leads to a greater proportion of mutants with intergenic lesions.

Effects of Radon and Radon Daughters on Human TK6 Lymphoblasts

We have begun to analyze the cytotoxic and mutagenic effects of ionizing radiation on human TK6 lymphoblasts. The cytotoxic effects of radon/radon daughters and X radiation are compared in Fig. 9. The radon/radon daughter dose used in this graph is that contributed by the medium only, since we have not as yet determined the dose contributed by the radon daughters attached to the cells. The cytotoxic effects for the human TK6 cells are similar to those shown previously for L5178Y lymphoblasts.

Fig. 9:
Cytoxic Effects of X radiation and Radon/Radon Daughters on TK6 Human Lymphoblasts

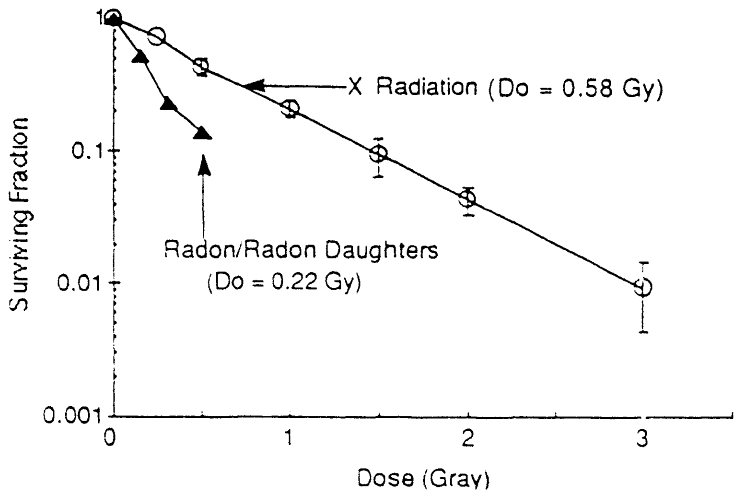

In preliminary experiments, exposure of human TK6 cells to 1.5 Gy X radiation resulted in 11% survival, and a mutant frequency of 193 x 10^{-6} at the *tk* locus. Slow-growing $TK^{-/-}$ mutants accounted for 70% of the mutant population. A much lower mutant frequency was obtained at the *hprt* locus following exposure to 1.5 Gy X radiation, amounting to only 11 x 10^{-6}. Exposure of TK6 cells to α radiation emitted by radon/radon daughters to give 53% survival resulted in a mutant frequency at the *hprt* locus of 6 x 10^{-6}. The mutant frequency remained at a similar level in this preliminary experiment as the exposure was increased to give 23% and 14% survival. Further experiments are planned in the near future to measure mutant frequency at the *tk* and *hprt* loci following exposure of TK6 cells to radon and radon daughters.

Nature of the Radiation-induced Lesion in the *hprt* gene in $HPRT^-$ Mutants of TK6 Cells

We have carried out molecular analysis of 4 spontaneous and 25 X radiation-induced $HPRT^-$ mutants. In the case of the spontaneous mutants, 2 were missing the entire *hprt* gene, 1 failed to yield a cDNA product upon reverse transcription of HPRT mRNA but showed exons 2-9 in the genomic DNA. The 4th spontaneous mutant harbored a splice mutation. Of the 25 X radiation-induced $HPRT^-$ mutants, 13 were lacking the entire *hprt* gene, 7 failed to yield a cDNA product, and 5 showed an mRNA product, 2 of which were of normal size, and 3 of which were smaller than normal. Of the 7 mutants failing to yield a cDNA product, 3 appeared to be missing exon 9 in the genomic DNA but exons 2-8 were present; the other 4 may be missing exon 1. In the case of the five mutants showing an mRNA product, the 2 giving mRNA of normal size may contain base change mutations or small deletions or insertions. Of the 3 showing small mRNA products, one had a base change mutation in a splice acceptor site which caused a deletion of 5 base-pairs in exon 2, one mutant was missing exon 2, and one mutant was missing exon 4. Further analyses of these and other HPRT⁻ mutants induced by X radiation and by radon/radon daughters will be carried out. We are especially interested in further study of the mutants which appear to be missing either exon 9 or exon 1, since these mutants may harbor deletions which extend into regions flanking the *hprt* gene and thus will be good candidates for the determination of deletion end points by the inverse polymerase chain reaction techniques outlined previously. We have recently isolated 11 independent radon/radon daughter-induced HPRT⁻ mutants which will be analyzed in a similar fashion.

Plans for 1992.

We will continue to isolate spontaneous HPRT⁻ mutants and those induced by X radiation and radon/radon daughters, and we will analyze the mutants in each group to obtain mutation spectra. One of the main objectives will be to determine the sequences found at the deletion endpoints of these mutants. Similar analyses will carried out at the heterozygous *tk* allele. The investigation of the effect of cell cycle stage at the time of irradiation on the nature of the mutational lesion will also be pursued.

END

DATE FILMED

01/09/92